

Deformation and Internal Force Variation Law of Cantilever Three-Row Pile Support Structure under the Condition of Pile-Soil Deformation Coordination

Tao Cheng^{1*}, Huan Zhang¹, Helong Chen¹, Dingbang Zhang¹, Yi Zhang²

¹School of Civil Engineering, Hubei Polytechnic University, Huangshi 435003, China

²Department of Civil Engineering, Tsinghua University, Beijing 100084, China

*Corresponding Author

Abstract:

At present, the three-row pile support structure is gradually used in engineering practice, but there is no mature calculation theory and design code for reference. To solve this problem, considering the coordination of pile-soil deformation, the three-dimensional finite element analysis of the three-row pile support structure is carried out, and the monitoring data of the actual project are compared to verify the rationality of the calculation method. On this basis, the effects of different factors (pile embedded depth, pile diameter, row spacing, pile spacing, excavation width, crown beam elastic modulus) on the deformation and stress of three rows of piles are studied. The numerical analysis results show that the embedded depth of three-rows piles should be $0.5h$ (H is the excavation depth of foundation pit), the pile diameter should be 400mm, and the row spacing and pile spacing should be $3d \sim 4d$ (d is the pile diameter). These laws provide a theoretical basis for the design and construction of a three-row pile support structure.

Keywords: *Existed workshop, Deep foundation pit, Cantilever row pile, Three-row pile support structure, Influential factor, Deformation compatibility, Internal force, Numerical simulation*

I. INTRODUCTION

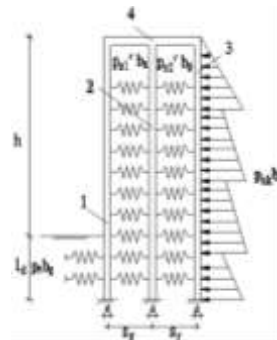
In recent years, as the scale of deep foundation pit grows increasingly large, the traditional double-row pile supporting structure fails to fully meet the needs due to the limitation of working environment. Compared with double-row piles, three-row piles have a greater lateral resisting stiffness^[1-2]. In the site environment with limited conditions such as the deformation of the pit working surface and the lateral deformation, three-row pile support structure has better adaptability. Therefore, three-row piles are gradually applied in the deep foundation pit engineering projects^[3-4].

Recently, the relatively mature calculation theories and specifications^[5-8] can be referred to for the single and double row pile calculation, but few research has focused on the triple row piles. Xin, et al.^[9] conducted the model test of the triple row piles, analyzed the deformation and the bending moment of the triple row piles through the test, and believed that the triple row piles had good antiskid effects. Compared with single row piles, its antiskid bearing capacity increased by 51.5% and could prevent great deformations of the slip mass. Xin, et al.^[10] combined the strength reduction method with the finite difference program FLAC3D and concluded the internal force distribution law of the triple row mini-piles under different landslide thrusts. Tian, et al.^[11] studied the deformation and the internal force of the triple row piles on the high and deep bank slopes of the waterway in a certain city, analyzed the influence rules of factors such as row spacing, pile stiffness and beam stiffness, and provided the reasonable design parameters such as row spacing, soil reinforcement positions, beam thickness, etc. Hu, et al.^[12] studied the variation law of the bank slope stability during the excavation in a canal bank slope restoration project which had the supporting structure of the triple-row bored piles. The results showed that: the construction quality of the triple-row bored piles played a very important role in the bank slope stability. Huang^[13] used the finite element method to analyze the deformation and internal force of the triple-row piles on a high slope, and made a comparative study on the influence of the length of the last two rows of piles. He believed that the front pile played a leading role, the rear two rows played a reverse anchoring role, and the piles in the middle row was weak in the lateral resisting movement. By combining the numerical simulation with the field monitoring, Zeng^[14] studied the laws about the deformation of the triple-row pile supporting structure and the pile top settlement, and proved that triple-row piles can effectively support the deformation of subways and tunnels.

At present, the research of the triple-row pile structure is mainly qualitative without the mature calculation theory. In order to solve this problem, the three-dimensional finite element method was used for the calculation and analysis of the triple-row pile support structure in this paper under the condition of considering the pile-soil deformation coordination. The monitoring data of the practical engineering were compared and the rationality of the calculation method was verified. Moreover, the law of deformation and internal force evolution under different working conditions was also further explored, which provided a theoretical basis for the design and construction of triple-row pile supporting structure.

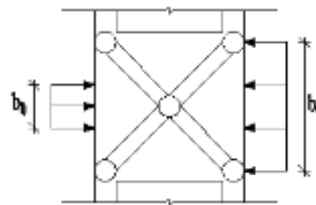
II. THEORETICAL MODEL

According to the stress characteristics of piles, the soil between piles is simplified as the soil springs^[15-16], and the bottom end of piles is regarded as the fixed end. The calculation model is shown in Fig 1. Accordingly, the calculated widths of active and passive earth pressure are shown in Fig 2.



1. Piles in the front row; 2. Piles in the middle row; 3. Piles in the last row; 4. Crown beam

Fig 1: Calculation model



b_0 -calculated width of passive zone; b_a - calculated width of active zone

Fig 2: Calculated width of earth pressure

The earth reaction acting on the front piles is calculated according to formula^[8] below.

$$p_s = k_s v + p_{s0} \tag{1}$$

Where, p_s is the soil reaction strength (kPa) of the front piles, k_s is the horizontal reaction coefficient of the soil (kN/m^3), which is calculated according to formula (2), v is the horizontal displacement of the front piles at the calculation point of the soil reaction (m), and p_{s0} is the initial soil reaction strength (kPa), calculated according to formula (3) ^[8].

$$k_s = m(z - h) \tag{2}$$

Where, m is the proportional coefficient of the soil's horizontal reaction coefficient (kN/M^4), which should be determined according to the field load test and the experience. Z is the distance from the calculation point to the ground (m). H is the excavation depth of the foundation pit (m).

$$p_{s0} = \sigma_{pk} K_{ai} \tag{3}$$

Where, σ_{ai} is the total vertical stress (kPa) generated by the soil's dead load at the calculation point inside the three rows of piles. K_{ai} is the pressure coefficient of the active soil. p'_{s1} is horizontal soil pressure of the soil between front and middle row piles on the inner side of the supporting structure.

$$p'_{s1} = k'_s \Delta v_1 + p'_{s0} \quad (4)$$

p'_{s2} is horizontal soil pressure of the soil between middle and rear row piles on the inner side of the supporting structure.

$$p'_{s2} = k'_s \Delta v_2 + p'_{s0} \quad (5)$$

Where, k'_s is the horizontal stiffness coefficient of the soil between piles (kN/m^3), calculated according to formula (6). Δv_1 is the horizontal displacement difference value between front and middle row piles (m). Δv_2 is the horizontal displacement difference value between middle and rear piles (m). p'_{s0} is the initial earth pressure (kPa) of the soil between piles on the pile side, calculated according to formula (7)^[17]. p'_{s1} is the pressure of the soil between front and middle rows of piles on the pile side (kPa); p'_{s2} is the pressure of the soil between middle and rear rows of piles on the pile side (kPa).

$$k'_s = \frac{E_s}{s_y - d} \quad (6)$$

Where, E_s is the calculated compression modulus (kPa) of the soil. s_y is the row spacing between three rows of piles (m). d is the diameter of the pile (m).

$$p'_{s0} = (2\alpha - \alpha^2) p_{ak} \quad (7)$$

$$\alpha = \frac{s_y - d}{h \tan(45^\circ - \varphi / 2)} \quad (8)$$

Where, α is the calculation coefficient. If $\alpha > 1$, and then $\alpha = 1$. φ is the internal friction angle of the foundation pit soil ($^\circ$). p_{ak} is the standard value of the active earth pressure strength at the calculation point of the outside soil mass for the three rows of piles, which is calculated according to formula (9)^[8].

$$p_{ak} = \sigma_{ak} K_a - 2c \sqrt{K_a} \quad (9)$$

Where, σ_{ak} is the total vertical stress (kPa) generated by the dead load of the soil at the calculated point outside the three rows of piles.

III. NUMERICAL ANALYSIS

3.1 Project Overview

The reconstruction project of a workshop is located in Huangshi, Hubei Province. The foundation pit excavation is required on the original ground of the workshop because of the reconstruction needs. The maximum excavation depth of the foundation pit is -9.0m, and the area is about 646m². The importance and safety level of the foundation pit is grade 2. Since the edge of the foundation pit is nearly 2m away from the edge of the workshop pillar, it is considered that the excessive lateral displacement of the workshop pillar may cause safety hazards. Therefore, the control requirements of the pit wall's lateral displacement were high and the spatial constraint effect was obvious during the foundation pit excavation. Meanwhile, because the heavy equipment base needed to be installed in the foundation pit, the small field operation surface made it impossible to set up the foundation pit support. Considering the excavation depth, the environmental conditions of the site and other factors, the traditional double-row pile structure failed to meet the requirements, and the three-row supporting structure was used. The pile diameter was 300mm, the row spacing between piles was 600mm, the pile length was 12.0m, and it was arranged in the shape of the quincunx. The top of the pile was C30 concrete beam, connecting the three rows of piles as a whole. Given the need of calculation, analysis and comparison, the parameters were monitored in real time and they included the horizontal displacement of the three-row pile supporting structure, the surrounding ground surface settlement, the foundation settlement of the workshop pillar, etc.

3.2 Model Parameters

The undisturbed soil of the foundation pit was taken for the relevant basic physical and mechanical tests according to literature^[18]. The related parameters of the soil were obtained and listed in TABLE I. According to the test parameters in TABLE I, the soil was the silty clay of medium compressibility and it was hard.

TABLE I. Physical and mechanical properties of soil

WATER CONTENT $w / (\%)$	DENSITY $\rho / (g/cm^3)$	PLASTIC LIMIT w_p	LIQUID LIMIT w_L	PLASTIC INDEX I_p	LIQUID INDEX I_L	COEFFICIENT OF COMPRESSIBILITY $a_{1-2} / (MPa^{-1})$	COMPRESSION MODULUS $E_s / (MPa)$	COHESIVE FORCE $c / (kPa)$	INTERNAL FRICTION ANGLE $\varphi / (^\circ)$	DILATANCY ANGLE $\psi / (^\circ)$
19.6	1.89	20.5	37.1	16.6	0.05	0.2	7.38	47.9	17.0	0

The geometric parameters of the calculation model for the foundation pit are as follows: The excavation depth of the foundation pit was 9m and the excavation width was 10m. In the 3D model, the excavation depth of the foundation pit in the vertical direction was enlarged 5 times (45m), and the excavation depth of the foundation pit in the horizontal direction was also enlarged 5 times^[19]. A three-row pile was taken as the calculation model (as shown in Fig.3 (a)), and the dimension of the model was 55m×45m×2.4m. The three-row pile support structure were arranged in a quincunx shape, and the calculation model is shown in Fig. 3. The geometric parameters of the support structure are shown in TABLE II.

TABLE II. Geometric parameters of three-row pile support structure

Pile length/m	Pile diameter/mm	Row spacing/mm	Pile spacing/mm	Crown beam section/mm
12	300	600	1200	150×400

In order to fully consider the pile-soil interaction, the solid elements were used for soil mass, piles and crown beams in the model. The linear elastic model was used for the three-row piles and the Mohr-Coulomb strength criterion was used for the soil mass. The tangential direction of the friction model on the pile-soil contact surface was the penalty function model, the friction coefficient was $\mu = \tan(0.75\varphi)$, φ was the internal friction angle of the soil mass, and the hard contact was selected in the normal direction^[20]. According to the geological survey report, little difference was shown in the soil layer of the foundation pit, which is mainly composed of silty clay. It was taken as the representative soil layer for calculation. The material parameters of soil mass, piles and crown beams are shown in TABLE III.

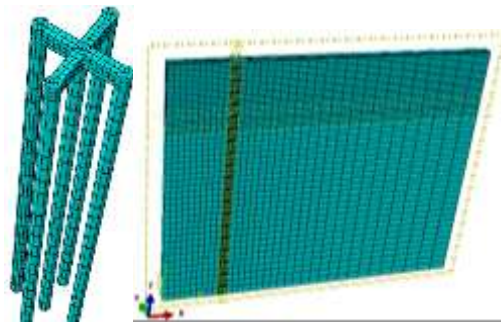
TABLE III. Physical and mechanical parameters of materials

Name	Density/ (kg/m ³)	Elastic modulus /MPa	Cohesive force /kPa	Internal friction angle/°	Poission ratio
Silly clay	1890	14.8	47.9	17	0.3
Piles and crown beams	2400	30000	-	-	0.2

3.3 Calculation Model

The element types of pile body, soil mass and crown beams were set as C3D8 (eight-node hexahedron element) to establish a 3D finite element calculation model. There were 50,520 elements in the soil mass, and 1,790 elements in the pile body. The grid division of the computing unit for the soil mass and pile body is shown in Fig 3.

The boundary conditions of the model are the constraints of the displacement in the X direction on the left and right sides, the displacement in the Y direction on the front and rear sides and the displacement in the X, Y and Z directions of the bottom. In this paper, keywords were used to define the initial ground stress method^[20] for the crustal stress balance. The method required the input of the coordinates of the highest and lowest point in different material areas as well as the dead weight stress. It is generally applicable to the geometric model with regular surface smoothness.



(a) pile body unit (b) soil mass unit

Fig 3: Finite element calculation grid of piles and soil

The steps of the simulated foundation pit excavation are as follows^[21] :

- 1) The finite element model of the soil mass, three-row piles and crown beams was established, the material got defined and the section was assigned attributes, and the components were assembled into a whole.
- 2) Three-rows piles were removed, and boundary conditions were set, and the weight of the soil mass was exercised to balance the initial ground stress.
- 3) The corresponding contact pairs of three-row piles and soil were activated.
- 4) The excavated soil mass was removed, and the contact pairs between three-row piles and the soil mass were deleted.

3.4 Validation of the Results

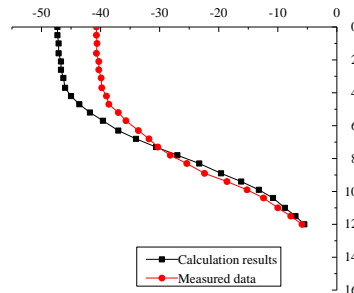


Fig 4: Comparison of horizontal displacement of pile

Fig 4 compared the calculated and measured values of the maximum pile displacements at different depths. As can be seen from Fig. 4, the numerical calculation result of the horizontal displacement at pile top was 47.3mm, while the measured data was 40.6mm. The variation trend of pile displacement got relatively close along with the variation trend of the depth. This indicated the rationality, reliability and applicability of the numerical calculation results in this paper.

IV. INFLUENCE OF DIFFERENT FACTORS

Based on the above calculation and analysis model, different factors (Embedded depth, pile diameter, row spacing between piles, etc.) were changed to analyze the change law of the pile displacement and the internal force and to study the mechanical mechanism of the three-row pile supporting structure. It provided a theoretical basis for establishing the calculation method of the three-row pile supporting structure.

4.1 Embedded Depth of Piles

Other factors (pile diameter, row spacing between piles, pile spacing, width of foundation pit excavation, etc.) were controlled and made constant. The different ratios of embedded depth and pile length were set to change the embedded depth of the pile support. The influence law of the pile's embedded depth on the three-row piles was explored Five working conditions are simulated, as shown in TABLE IV.

TABLE IV. Embedded depth of pile

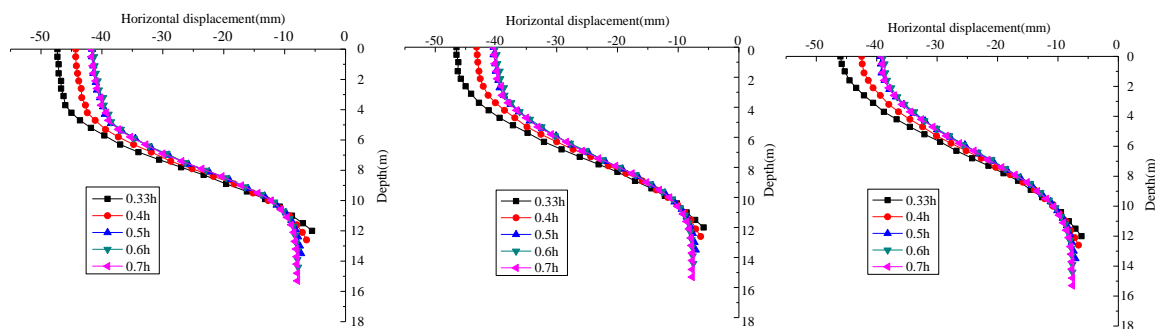
Working conditions	1	2	3	4	5
Embedded depth	0.33h	0.4h	0.5h	0.6h	0.7h

Notes: h is the excavation depth of the foundation pit(m).

Fig 5 shows the calculated results of the horizontal displacement under five different working conditions. The variation trend of horizontal displacement in front, middle and rear piles was basically the same: under the same embedded depth, the maximum horizontal displacement of the three-row piles ranked as follows: front pile > middle row pile > rear pile. Under the foundation pit subface, the displacement changed little when the embedded depth got changed. The maximum horizontal displacement of front, middle and rear piles decreased gradually with the increase of embedded depth. However, when the embedded depth reached 0.5h, the maximum horizontal displacement didn't change much. Therefore, 0.5h can be regarded as the design threshold of the embedded depth.

Fig 6 shows the bending moment of the pile section under different working conditions. The embedded depth didn't obviously influence the maximum negative bending moment of front, middle and rear piles. The maximum negative bending moment of front middle piles was at about 10m, and the maximum positive bending moment was at about 5-6m. The maximum positive bending moment of the rear pile was at the pile top, while the maximum negative bending moment was at the bottom of the pit. The maximum bending moment of middle piles was smaller than that of front and rear piles, so in the practical engineering design, it can be considered that the piles in front and rear rows should be equipped with more bending reinforced bar than middle piles.

In conclusion, increasing the embedded depth can reduce the horizontal displacement of piles to a certain extent. However, when the embedded depth exceeded a certain threshold, it had little effect on reducing the horizontal displacement of the supporting structure and would increase the economic cost. Therefore, the recommended design value of the embedded depth for the three-row piles can be set as 0.5h.

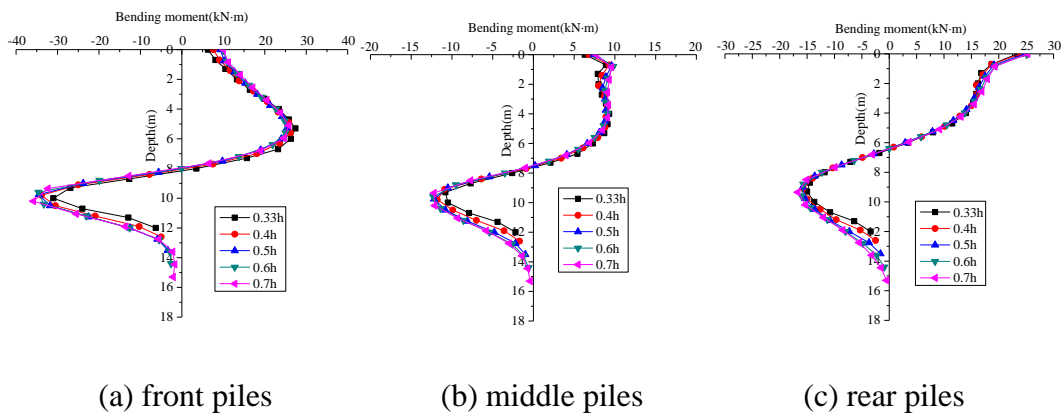


(a) front piles

(b) middle piles

(c) rear piles

Fig 5: Relationship curve between horizontal displacement and embedded depth



(a) front piles (b) middle piles (c) rear piles
 Fig 6: Relationship curve between section bending moment and embedded depth

4.2 Pile Diameter

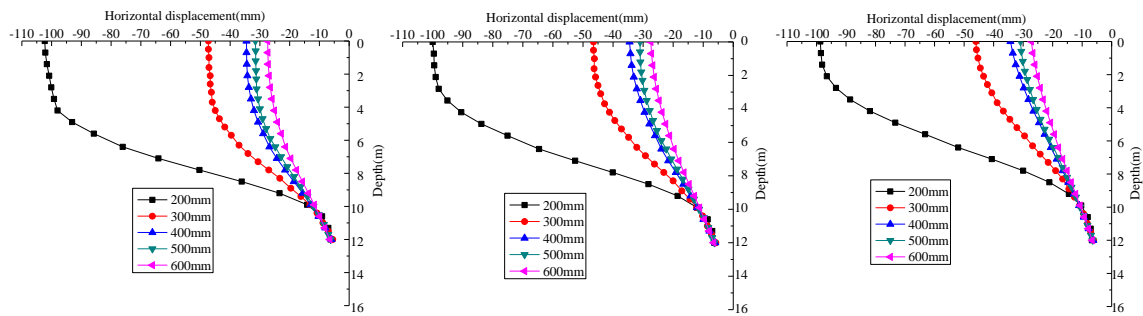
In order to study the influence rule of the pile diameter, and five possible pile diameters were selected for calculation based on the engineering practice, as shown in TABLE V.

TABLE V. Pile diameter (mm)

Working conditions	1	2	3	4	5
Pile diameter	200	300	400	500	600

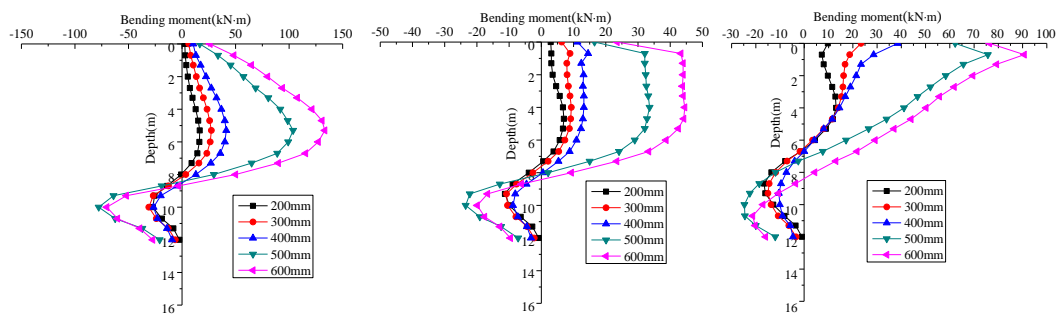
Fig 7 and Fig 8 are relationship curves of the maximum horizontal displacement and the section bending moment that changed along with pile diameters. As can be seen from the Fig, the maximum horizontal displacements of front, middle and rear piles all decreased with the increase of pile diameters, while the maximum positive bending moment increases with the increase of pile diameters. However, when the pile diameter was between 200mm and 400mm, the maximum horizontal displacement of the pile decreased rapidly and the maximum positive bending moment increased slowly as the pile diameter increased. When the pile diameter was between 400mm and 600mm, the maximum horizontal displacement of the pile decreased slowly with the increase of the pile diameter, while the maximum positive bending moment increased rapidly.

In conclusion, the structural stiffness of the three-row piles increased with the increase of the pile diameter. 200mm~400mm is the recommended range of designing the pile diameter, and 400mm is the critical point of stiffness, namely the design threshold of the pile diameter.



(a) front piles (b) middle piles (c) rear piles

Fig 7: Relationship curve between horizontal displacement and pile diameter



(a) front piles (b) middle piles (c) rear piles

Fig 8: Relationship curve between section bending moment and pile diameter

4.3 Row Spacing of Piles

In the engineering design of the three-row piles, the change of row spacing will affect the distribution form of the earth pressure in front, middle and rear piles. In order to determine more reasonable row spacing and make other factors constant, five different row spacing conditions were simulated as shown in TABLE VI.

TABLE VI. Row spacing of pile (mm)

Working conditions	1	2	3	4	5
Row spacing	2d	3d	4d	5d	6d

Fig 9 shows the horizontal displacement changes along with the row spacing. The front pile was less affected by row spacing, and its displacement was closer under different row spacings. However, the middle and rear piles were greatly affected by it. The maximum horizontal displacement of front, middle

and rear piles decreased with the increase of row spacing. When the row spacing changed from 3d to 4D, the maximum horizontal displacement decreased gently.

Fig 10 shows the bending moment changes along with the row spacing. For front piles, with the increase of row spacing, the maximum bending moment increased gradually but with an increasingly small trend. The maximum positive bending moment of middle row piles increased gradually with the increase of row spacing, while the negative bending moment increased first and then decreased. With the increase of row spacing, the reverse bending point gradually moved up, indicating that: with the increase of row spacing, middle rows produced an increasingly strong Rachel effect on front piles. In general, the maximum positive bending moment of the front, middle and rear piles increased with the increase of row spacing. When the row spacing was from 3d to 4d, the maximum positive bending moment of the front and rear piles showed relatively small differences, and the stress was relatively uniform, which can give full play to the role of each piles in row.

In conclusion, the recommended range of the three-row piles was 3d-4d.

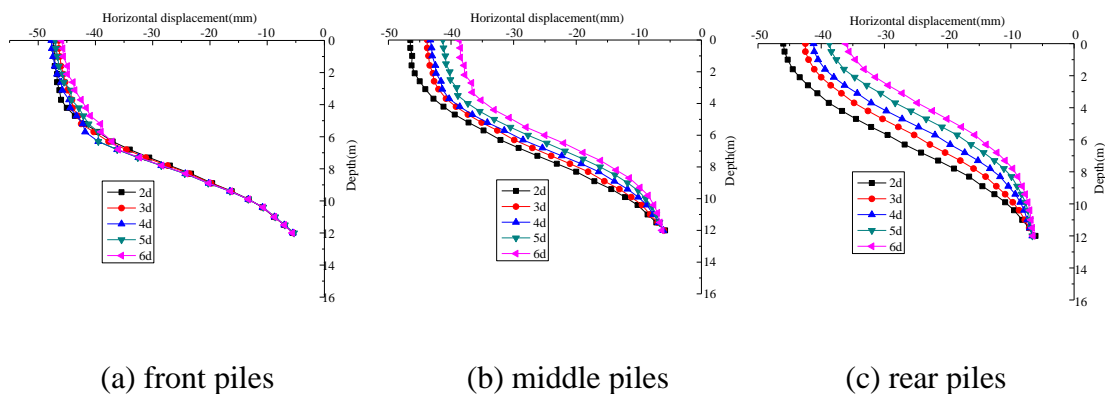


Fig 9: Relationship curve between horizontal displacement and row spacing

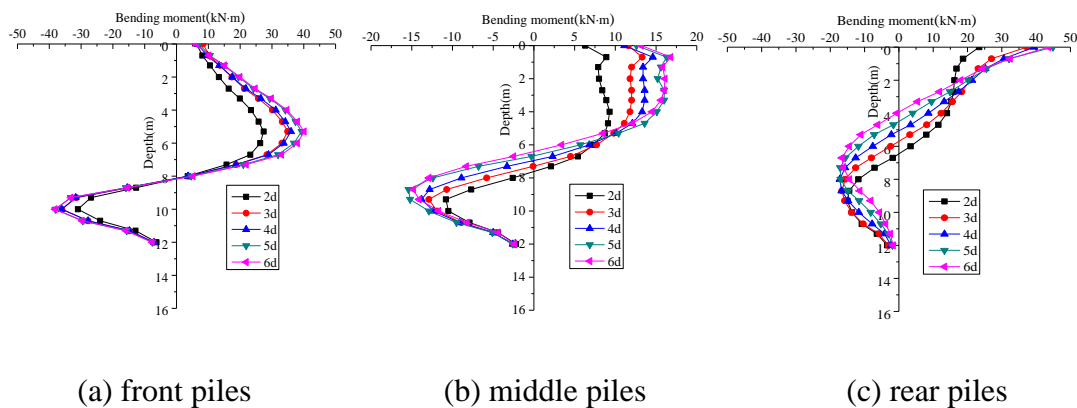


Fig 10: Relationship curve between section bending moment and row spacing

4.4 Pile Spacing

To analyze the influence law of the pile spacing, five different working conditions were used, as shown in TABLE VII.

TABLE VII. Pile spacing

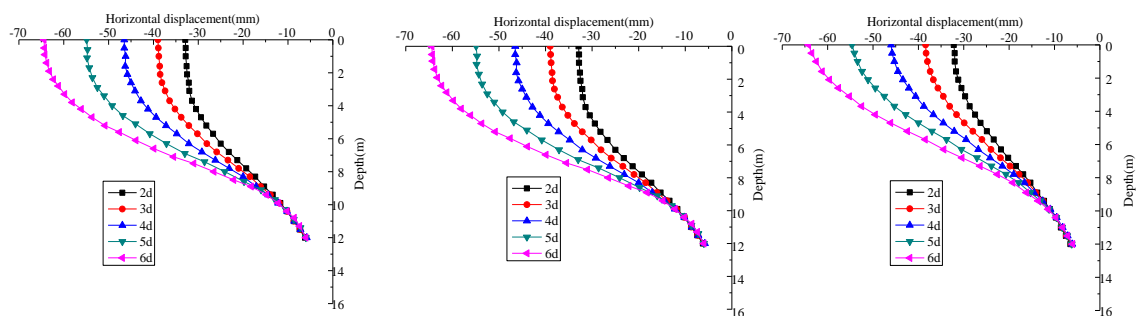
Working conditions	1	2	3	4	5
Pile spacing	2d	3d	4d	5d	6d

Notes: d is the pile diameter.

Fig 11 shows the horizontal displacement changes along with pile spacing. The pile body’s horizontal displacement of three-row piles increased at a growing rate with the increase of pile spacing. When the pile spacing was between 2d and 4d, the maximum horizontal displacement difference of front, middle and rear piles was relatively small. Below the foundation pit subface (below 9m), the displacement was almost unchanged due to the good embedment of the soil.

Fig12 shows the bending moment changes along with pile spacing. As the pile spacing increased, the maximum positive and negative bending moments of three-row piles also increased at a growing rate. The inflection points of the front and middle row piles were close to each other, and they were located about 8m underground. However, the pile body’s inflection point of rear piles moved up, indicating that the excessive pile spacing will cause the soil deformation of the lateral pile, causing an increase in the internal force and the supporting structure deformation. When the pile spacing was from 3d to 4d, the maximum positive bending moment of middle and rear piles changed little, and the stress of middle and rear piles was relatively uniform.

The increase of pile spacing will cause the displacement and internal force of the supporting structure to increase, which is likely to cause the instability of the supporting structure. However, the smaller pile spacing will increase the number of piles, resulting in excessive economic cost. Based on the above analysis, the recommended design range of the three-row pile spacing of is 3d ~ 4d.



(a) front piles

(b) middle piles

(c) rear piles

Fig 11: Relationship curve between horizontal displacement and pile spacing

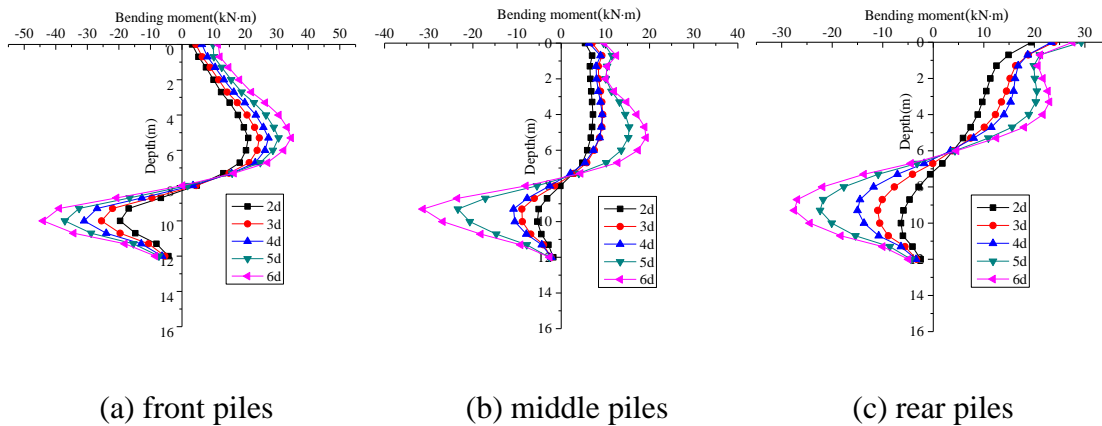


Fig 12: Relationship curve between section bending moment and pile spacing

4.5 Excavation Width

To analyze the influence law of the excavation width, four different working conditions were used, as shown in TABLE VIII.

TABLE VIII. Excavation width of foundation pit (m)

Working conditions	1	2	3	4
Excavation depth	10	20	30	40

Fig 13 shows the horizontal displacement changes along with the excavation depth of the foundation pit. The horizontal displacement of the three-row piles increased along with the increase of excavation width, and the maximum horizontal displacement was at the pile top. The influence degree of the foundation pit excavation width on the supporting structure of three-row piles tended to increase slowly. When the excavation width was 10m ~ 20m, the displacement of three-row piles didn't change obviously.

Fig 14 shows the bending moment changes along with the excavation width of the foundation pit. The bending moment of the three-row piles was less affected by the excavation width of foundation pit, because the overall lateral resisting stiffness of the three-row piles was large, and the coordinated distribution of internal forces was strong. Therefore, the internal force changed little.

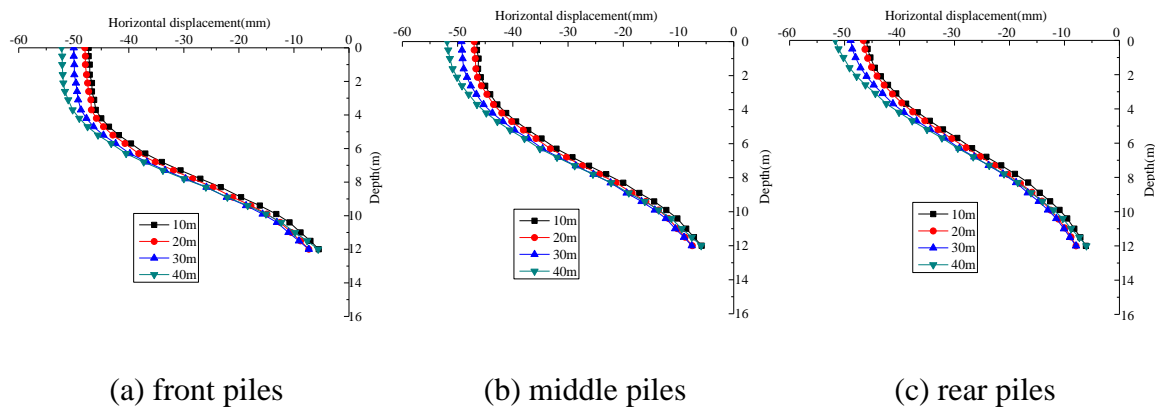


Fig 13: Relationship curve between horizontal displacement and excavation depth

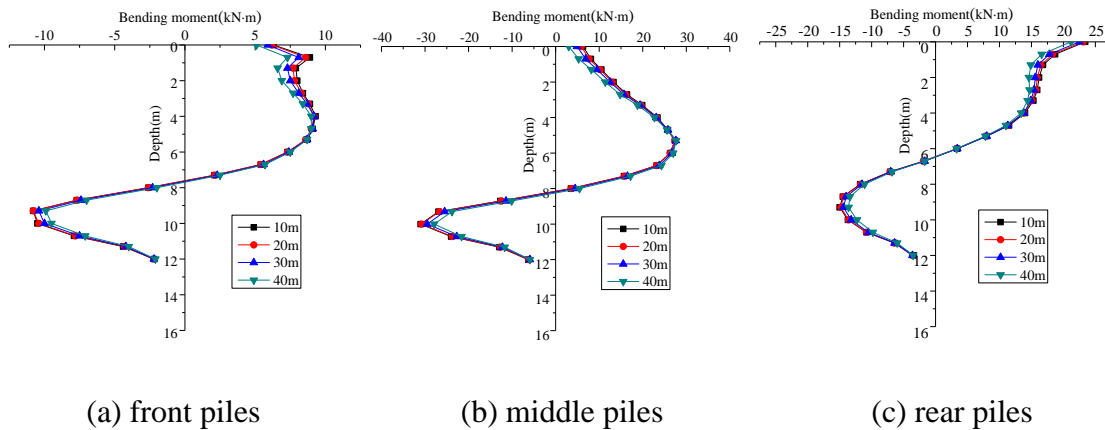


Fig 14: Relationship curve between section bending moment and excavation width

4.6 Crown Beam Stiffness

To study the influence law of the crown beam stiffness, three different working conditions were used, as shown in TABLE IX.

TABLE IX. Elastic modulus of crown beam

Working conditions	1	2	3
Elastic modulus of crown beam/(GPa)	0.5E	1E	1.5E

Notes: E is the elastic modulus of the pile body.

The horizontal displacement changes along with the elastic modulus of crown beam, as shown in Fig 15. As the elastic modulus of crown beam increased, the pile displacement gradually dropped at a decreasing rate. The bending moment change curve of the pile body is shown in Fig 16, and changing the elastic modulus of crown beam didn't obviously influence the bending moment change of three-row piles. Therefore, it can be known that: the supporting effect enhancement for the three-row piles was not obvious

by increasing the elastic modulus of the crown beam, which also indicates that the three-row pile structure is good in terms of lateral resisting stiffness and overall stability.

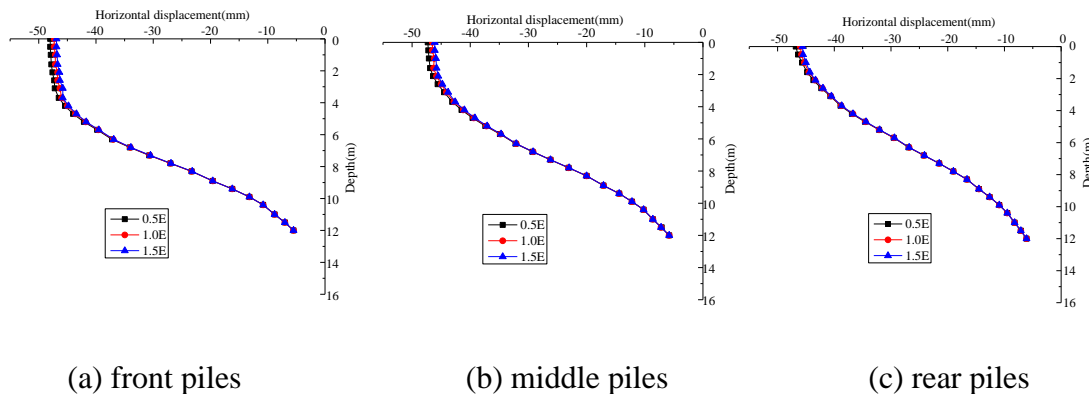


Fig15: Relationship curve between horizontal displacement and elastic modulus of crown beam

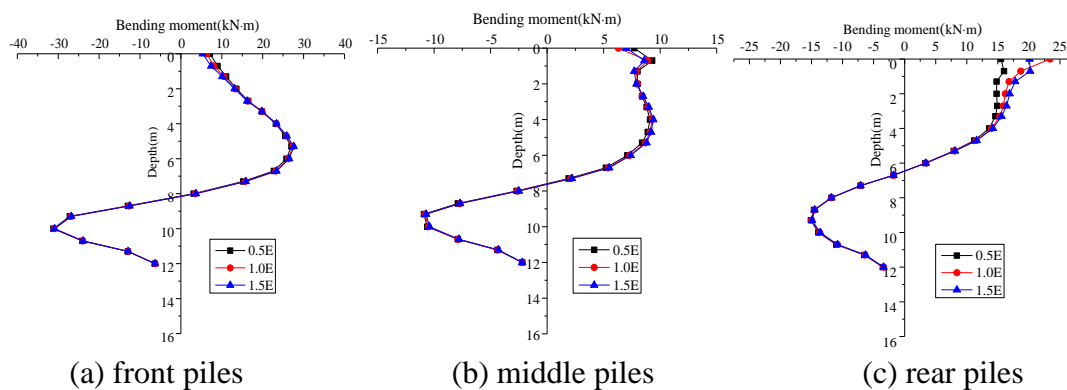


Fig 16: Relationship curve between section bending moment and elastic modulus of crown beam

V. CONCLUSIONS

Based on the pile-soil displacement coordination, a three-dimensional finite element model for three-row piles was established in this paper, and its rationality got verified by comparing the simulated data with the measured data. On this basis, the influence law of different factors on the deformation and internal force of three-row piles was simulated, which provided the theoretical basis for the design and construction of three-row piles. The following conclusions are drawn:

- 1) The horizontal displacement of the supporting structure can be reduced by increasing the pile's embedded depth (i.e. increasing the pile length), and the optimum embedded depth of three-row piles should be 0.5h (h is the excavation depth of the foundation pit).
- 2) Increasing the pile diameter can improve the pile stiffness and reduce the horizontal displacement of the supporting structure. When the pile diameter exceeded 400mm, the displacement of three-row piles

didn't decrease obviously. 400mm can be used as the threshold of the designed pile diameter, and 200mm~400mm was the recommended range of the designed pile diameter.

3) When the row spacing changed in between 3d and 4d, the maximum positive bending moment of front and rear piles were relatively small, and the maximum horizontal displacement decreased gently. Therefore, it is suggested that the design range of the row spacing for three-row piles is 3d~4d.

4) When the pile spacing varied from 2d to 4d, the maximum horizontal displacement difference of threerow piles was relatively small, and the maximum positive bending moment of middle and rear piles changed little. Therefore, the recommended design range of the pile spacing for three-row piles is 3d~4d.

5) The excavation width of the foundation pit and the stiffening of crown beam had a certain influence on the displacement and internal force of the supporting structure, but it was not significant.

ACKNOWLEDGEMENTS

The study was supported by the Program for Science and Technology Innovation Team in Colleges of Hubei Province (CN) under Grant T201823, the Natural Science Foundation of Hubei Province (CN) under Grant 2012FKC14201, the Scientific Research Foundation of Education Department of Hubei Province (CN) under Grant D20134401, the Natural Science Foundation of Hubei Polytechnic University under Grant 13xjz03A. Their financial support is gratefully acknowledged.

REFERENCES

- [1] Brown D. A., Shie C. F. (1990). Numerical experiments into group effects on the response of piles to lateral loading. *Comput. Geotech.*, 10(3): 211–230.
- [2] Hwang T. H., Kim K.H., Shin J. H. (2017). Effective installation of micro piles to enhance the bearing capacity of micropile draft. *Soils & Foundations*, 57(1): 36–49.
- [3] Cao Z. (2017). Research on internal force and deformation of retaining structure with treble-row piles in deep foundation pit. Wuhan University of Technology.
- [4] Dong J.H., Zhuang C. (2019). Mechanical properties analysis on frame prestressed anchor micro steel tube pile combined retaining structure of deep foundation pit. *Chinese J. Rock Mech. Eng.*, 38(03): 619-633.
- [4] Wang Z.H., Zhou J. (2011). Three-dimensional numerical simulation and earth pressure analysis on double-row piles with consideration of spatial effects. *J. Zhejiang Univ.-Sci. A: Appl. Phy. & Eng.*, 12(10):758-770.
- [5] Yang G. H., Huang Z. M., Jiang Y., et al. (2016). Improvement of calculation model of double-row piles for supporting deep excavation. *Rock Soil Mech.*, 37(S2): 1–15.
- [6] ZHENG Gang, LEI Ya-wei, CHENG Xue-song, et al. (2019). Experimental study of the influence of local failure on steel strutted pile retaining system of deepexcavation. *Chinese Journal of Geotechnical*

Engineering, 41(8): 1390-1399.

- [7] JGJ120-2012. (2012). Technical specification for retaining and protection of building foundation excavations. China: Architecture & Building Press.
- [8] Xin J.P., Tang X.S., Zheng Y. R., et al. (2015). Large-scale model tests of single-row and triple-row anti-slide micropiles. *Rock Soil Mech.*, 36(4): 1050–1056.
- [9] Xin J.P., Zheng Y. R., Tang X. S., et al. (2012). Numerical simulation of internal force distribution of three-row micropiles. *Chongqing Arch.*, 11 (9):71-75.
- [10] Tian Z.Q, Shen B.G. (2016). Study on the structural characteristics and calculation methods of three-row pile support. *China Water Transport*, 37(9):73-75.
- [11] Hu Z., Liu N. S., Jin Y. (2017). Study on the Stability of Deep Slope with Three-row Piles Supporting. *Constr. Tech.*, 46 (5):20-24.
- [12] Huang W. D. (2017). Performance and simplified calculation of three-row pile of high slope stability retaining structure. *Geotechnical Investigation & Surveying*, 45(12):9-14.
- [13] Zeng S. Y. (2019). Analysis of Influence of Deep Foundation Pit Construction with Three-row Pile Isolation Support on Existing Rail Transit. *Soil Eng. Found*, 33(02):103-106.
- [14] Terzaghi K. (1943). *Theoretical soil mechanics*. New York: John Wiley & Sons.
- [15] Paik K. H., Salgado R. (2003). Estimation of active earth pressure against rigid retaining walls considering arching effects. *Géotechnique*, 53(53):643-653.
- [16] Cheng Y. M., Hu Y. Y., Wei W.B. (2007). General Axisymmetric Active Earth Pressure by Method of Characteristics-Theory and Numerical Formulation. *Int. J. of Geomech*, 7 (1):1-15.
- [17] GB/T50123-1999. (1999). Standard for geotechnical testing method. China Planning Press.
- [18] Bransby P. L., Smith I.A.A. (1975). Side Friction in Model Retaining-Wall Experiments. *Journal of the Geotechnical Engineering Division, ASCE*, 101(GT7):615-632.
- [19] Wei S. S. (2015). Analysis of deformation factors in the deformation of the double-pile support system in the deep pit. Master Thesis, Tianjin University.
- [20] Li J. Q. (2011). Analysis of factors affecting the calculation of deformation of pit foundation support design in pits. Master Thesis, Tianjin University.